RAPID COMMUNICATIONS

PHYSICAL REVIEW E VOLUME 50, NUMBER 2 AUGUST 1994

# Structure in the electric potential emanating from DNA

Glenn Edwards, David Hochberg, and Thomas W. Kephart
*Department of Physics and Astronomy, Vanderbilt University, Nashville, Tennessee 37235*
(Received 13 June 1994)

We present an analytical model, based on a Green-function technique, for the electric potential surrounding dissolved DNA which treats the full, discrete charge distribution of homopolymer *B*-DNA and the aqueous solvent as concentric, dielectric cylinders. The resulting expressions manifest the symmetry of the system, with terms equivalent to a continuous line charge and with distinctive helical terms both due to the sugar-phosphate backbone and due to the base pairs. This theoretical approach quantifies the structural information in the potential with continuing approach to the DNA surface.

PACS number(s): 87.15.−v, 36.20.−r, 41.20.Cv

An *ab initio* calculation of the electric potential and field for dissolved DNA is currently an intractable problem. In the past a number of idealizations have been used to model the thermodynamic and electrostatic properties of DNA, with emphasis either on the solvent [1–4] or on the structural details of DNA [5]. Another class of models treats in detail both DNA and the solvent [6,7], but the size of the system is limited by computational power. In general, each class of models exhibits definite but limited reliability in addressing this complex problem.

Here we report the results of our theoretical investigation of the structural information retained in the electric potential. While the dominant charges of DNA are the phosphate groups, a nucleotide pair (unit cell) has either 45 (deoxyadenylic acid–deoxythymidylic acid) or 46 (deoxyguanylic acid–deoxycytidylic acid) partially charged atoms [8]. Here we model homopolymer *B*-DNA by taking into account each atom as a partial charge at its atomic coordinate. We have used partial charges from Renugopalakrishnan, Lakshminarayanan, and Sasisekharan [9] for the backbone and from Pearlman and Kim [10] for the bases in the parameters determined by Arnott and Hukins [11]. In addition to the DNA macromolecule, concentric regions of condensed ions and bulk solvent are modeled as dielectric media with cylindrical symmetry. Initially we modeled the solvent as three dielectric regions as shown in Fig. 1(a), where $b$ is the DNA radius. While the phosphate groups are essentially bound surface charges, counterions and other solvent ions are free charges. Surrounding the polyelectrolyte DNA is a region of condensed ions known as the Manning layer [12–14], modeled as the cylindrical shell from $b$ to $d$ in Fig. 1(a). In biological systems this region is at a molarity of about 2 independent of the molarity of the surrounding bulklike solvent, which is typically tens of millimolars.

Recently we solved the problem of the local electric field that arises from the phosphate groups using a Green-function technique, i.e., a helical charge distribution in concentric dielectric media, pointing out that the full power of the Green-function approach is required for analytical solutions [15]. While limiting the charges to that of the phosphate groups successfully identified a helical "signature," it failed to recognize the partial charge distribution of the sugars and the bases. Here we extend the theory to a more realistic model for DNA. We have considered using the multipole expansion to account for the sugars and especially the bases. However, a comparison of the relative contributions from subsequent terms in the expansion, at length scales relevant to this system, indicates that the dipole approximation is not always valid and the multipole expansion is not a useful approach for the region manifesting structural information.

Given the linearity of Maxwell's equations we have taken a reductionist approach to build up the potential due to the full charge distribution. Let us focus our attention on deriving $\Phi_2$, the potential in the Manning region (the development of the potential in the other two regions makes use of similar manipulations). First consider a point charge at a dielectric boundary as shown in Fig. 1(a). It is straightforward to show [15] that the potential is given by

$$\Phi_2(\rho,\phi,z)=\frac{4q}{b}\frac{1}{\pi}\sum_{m=0}^{\infty'}\int_0^{\infty}\frac{dk}{k}B_{m,k}[r_{(m,k)}I_m(k\rho)+K_m(k\rho)]$$

$$\times\cos[k(z-z')]\cos[m(\phi-\phi')],$$

for $b<\rho<d$, where the prime on the sum indicates the $m=0$ term is divided by 2, and

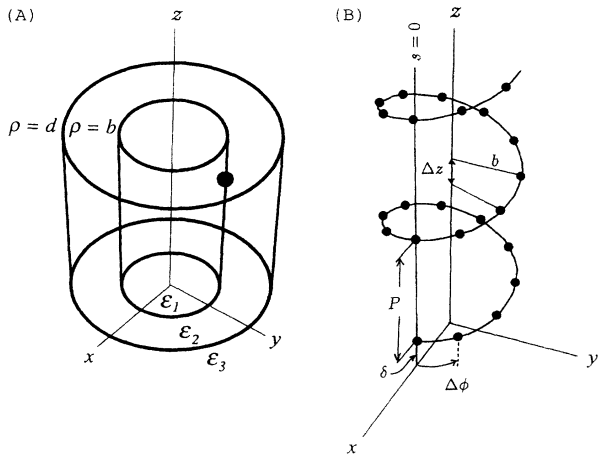


FIG. 1. (a) Geometry for a single phosphate embedded in three concentric dielectric media (three-layer model). (b) Cylindrical surface containing the lattice of charges associated with one helix of phosphates.

 

$$B_{m,k} \equiv \frac{I_m(kb)}{(\epsilon_1-\epsilon_2)r_{(m,k)}I'_m(kb)I_m(kb)+[\epsilon_1 I'_m(kb)K_m(kb)-\epsilon_2 K'_m(kb)I_m(kb)}\,,$$

$$r_{(m,k)} \equiv \frac{(\epsilon_2-\epsilon_3)K'_m(kd)K_m(kd)}{\epsilon_3 I_m(kd)K'_m(kd)-\epsilon_2 I'_m(kd)K_m(kd)}\,.$$

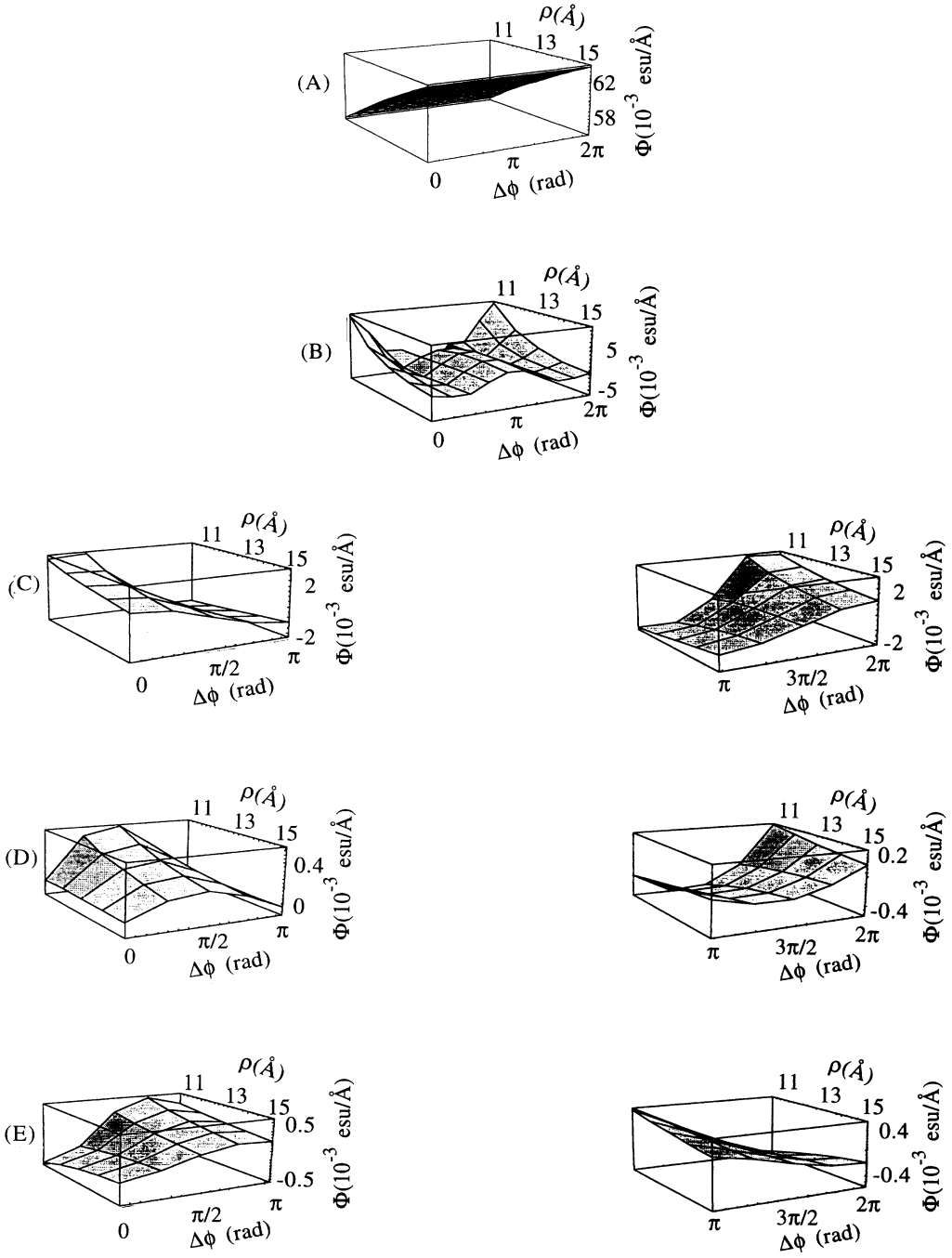


FIG. 2. Surface plots ($z=0$ plane) of the terms comprising the electric potential: (a) zero mode; nonzero mode contributions for the (b) phosphate groups, (c) ribose groups, (d) guanine, and (e) cytosine. Computations were performed as described in Ref. [15]. Note the radius is 1–4 Å from the DNA surface ($b=10$ Å).

$I_m$ and $K_m$ are the two linearly independent modified Bessel functions of order $m$. The sum on $m$ reflects a discrete Fourier expansion in $\phi$, while the $z$ dependence is handled with a continuous Fourier expansion (integration over $k$). Note the difficulty associated with computing the sums and integrals of the products of multiple modified Bessel functions. The resolution to this difficulty is found by recognizing the symmetries of DNA and decomposing the helical charge distribution into a set of ten lines of discrete charges as shown in Fig. 1(b). More specifically, the position of the $n$th charge on the $s$th line (with fixed angular coordinate $\phi_s$) is $(b,\phi_s,z_{n,s})$, where

$$z_{n,s}=nP+s\Delta z,$$

$$\phi_s=\left(\frac{2\pi}{N_0}\right)s,$$

with $0\leq s\leq(N_0-1)$ and $-\infty<n<\infty$ and where $P$ is the helix pitch and $\Delta z$ is the rise per residue as shown in Fig. 1(b). The sum on $n$ (for fixed $s$) builds up one line of discrete charges and is effected by means of the Poisson summation formula [16]:

$$\sum_{n=-\infty}^{\infty}\cos\{k[z-(nP+s\Delta z)]\}$$

$$=\frac{2\pi}{P}\cos[k(z-s\Delta z)]\sum_{j=-\infty}^{\infty}\delta\left(k-\frac{2\pi j}{P}\right),$$

where this $\delta$ function will trivialize the integrals in the potential equations, reducing them to a form that is computationally tractable. Let $\Phi_2^s$ represent the contribution from a single line of discrete charges. It will be convenient both conceptually and computationally to split off the zero mode ($m=0$, $k=0$) contribution from the higher-mode terms:

$$\Phi_2^s=\Phi_2^s(m=0,k=0)+\Phi_2^s(m=0,k>0)$$
$$+\Phi_2^s(m\geq 1,k=0)+\Phi_2^s(m\geq 1,k>0).$$

Each mode reflects coherence in the electric potential, where the $m$ modes are periodic in angular separation and the $k$ modes are periodic in the $z$ direction [note that $k\sim(2\pi/P)$ for a pitch $P$].

It is straightforward to build up the contribution to the potential by a lattice of atoms as shown in Fig. 2(b) by summing over all $s$. Note that this lattice defines a cylindrical surface. Although the double-helix configuration of point charges does *not* possess cylindrical symmetry, the lattice of, for example, phosphates can be located on a single cylindrical surface and thus our separation of Laplace's operator in cylindrical coordinates is natural indeed.

Recall that the second interface at $\rho=d$ corresponds to the outer extent of the Manning region. We have quantified the reflection from the dielectric layer at $\rho=d$ and it is insignificant. While the phosphate charges are taken to lie at the DNA surface, rescaling $b$ allows the lattice of atoms in Fig. 1(b) to represent the lattice associated with any atom in the nucleotide pair. Apart from its radius, the helical lattice geometry is uniquely characterized by the helix pitch $P$ and the vertical rise per residue $\Delta z$. Given the three-layer potential, it is a simple matter to obtain the potential for an infinite helical charge distribution for a two-layer dielectric, where a given charge lies entirely within the first ($\epsilon_1$) layer. We can then build up the electrostatic potentials associated with the various chemical structures making up the complete DNA macromolecule. To obtain the potential from an infinite helix of identical *base pairs*, we simply rescale the radius $a\rightarrow a_j$ and charge $q\rightarrow q_j$, shift angles and altitudes $\phi\rightarrow\phi+\alpha_j$, $z\rightarrow z+\delta_j$ for each atomic partial charge residing in the given base, and then separately sum over all the constituent atoms belonging to each base:

$$\Phi_{G\text{-}C}(\rho,\phi,z)=\sum_{j=1}^{15}\Phi^j_{2,\text{helix}}(\rho,\phi+\alpha_j^c,z+\delta_j^c)$$
$$+\sum_{j=1}^{12}\Phi^j_{2,\text{helix}}(\rho,\phi-\alpha_j^G,z-\delta_j^G),$$

where the sums over 15 and 12 correspond to the separate guanine and cytosine bases, respectively, and the superscript $j$ on $\Phi$ labels the cylindrical shell containing $q_j$. In contrast, for the *sugar-phosphate backbone* we add the dyadically related groups before performing the sum over the constituent partial atomic charges:

$$\Phi^j_{\text{double helix}}(\rho,\phi,z)=\Phi^j_{\text{helix}}(\rho,\phi+\alpha_j,z+\delta_j)$$
$$+\Phi^j_{\text{helix}}(\rho,\phi-\alpha_j,z-\delta_j).$$

For a given *backbone* charge $q_j$, the contribution to the potential has the form

$$\Phi^j_{\text{double helix}}(m=0,k=0)=-2N_0\frac{2q_j/\epsilon_2}{P}\ln(\rho),$$

$$\Phi^j_{\text{double helix}}(m=0,k>0)=\frac{2q_j}{b\pi}\sum_{l=1}^{\infty}\frac{1}{l}2\cos\left(\frac{2\pi l}{\Delta z}z\right)\cos\left(\frac{2\pi l}{\Delta z}\delta_j\right)\wp^j_{0,2\pi l/\Delta z}K_0\left(\frac{2\pi l}{\Delta z}\rho\right),$$

$$\Phi^j_{\text{double helix}}(m\geq 1,k=0)=\frac{4q_j}{P}\sum_{l=1}^{\infty}\frac{1}{l}2\cos(lN_0\phi)\cos(lN_0\alpha_j)\left(\frac{\frac{\epsilon_1-\epsilon_2}{\epsilon_2(\epsilon_1+\epsilon_2)}+1}{2\epsilon_1}\right)\left(\frac{a_j}{\rho}\right)^{lN_0},$$

$$\Phi^{j}_{\text{double helix}}(m\geq 1,k>0)=\frac{2q_jN_0}{b\pi}\sum_{l=1}^{\infty}\sum_{m=1}^{lN_0-1}2\cos\left(\frac{2\pi z}{P}(lN_0-m)+m\phi\right)\cos\left(\frac{2\pi\delta_j}{P}(lN_0-m)+m\alpha_j\right)$$

$$\times\frac{1}{lN_0-m}\wp^{j}_{m,(2\pi/P)(lN_0-m)}K_m\left(\frac{2\pi}{P}(lN_0-m)\rho\right)+\frac{2q_jN_0}{b\pi}\sum_{l=-\infty}^{\infty}\sum_{m=\max[1,1-lN_0]}^{\infty}2\cos\left(\frac{2\pi z}{P}(lN_0+m)-m\phi\right)$$

$$\times\cos\left(\frac{2\pi\delta_j}{P}(lN_0+m)-m\alpha_j\right)\frac{1}{lN_0+m}\wp^{j}_{m,(2\pi/P)(lN_0+m)}K_m\left(\frac{2\pi}{P}(lN_0+m)\rho\right),$$

where we have made use of the definition

$$\wp_{(m,k)}\equiv\frac{I_m(ka)}{\epsilon_1 I'_m(kb)K_m(kb)-\epsilon_2 I_m(kb)K'_m(kb)}.$$

As expected, the resulting analytical expressions manifest the symmetry of the system. For each chemical structure the leading term ($m=0$, $k=0$) is equivalent to a continuous line charge as shown in Fig. 2(a); we refer to the sum of these leading terms as the zero mode. A subset of higher-order terms due to the sugar-phosphate backbone have a characteristic length scale of 5 Å beyond the DNA surface as shown in Figs. 2(b) and 2(c). Another subset of higher-order terms are due to partial charges of the bases and have a characteristic length scale of several angstroms beyond the DNA surface as shown in Figs. 2(d) and 2(e). These higher-order "corrections" to the logarithmic term make significant contributions to the electrostatic potential near the DNA surface and represent the "signatures" in the potential for both the double helix and specific bases.

At distances far from the surface the electric potential due to DNA limits to that of a continuous line charge, as required. With continuing approach the nonzero modes begin to contribute, first as a helical signature and then with base-specific structural information. Inspection of Fig. 2 indicates that the gradients of the nonzero modes dominate those of the zero mode near the DNA-solvent interface. Care must be taken, however, in interpreting the results of any idealized model, including this one [15].

In summary, we have presented an analytical solution for the electric potential due to the complete microscopic charge distribution of dissolved *B*-DNA. This result is relevant to experimental efforts to image nucleic acids with atomic force microscopy [17] and to experimental, theoretical, and computational investigations of intermolecular interactions and diffusional encounter in general [7,18]. We plan to extend our investigation, incorporating more sophisticated models of the surrounding solvent [18] and to merge this analytical solution with computational methods to gain insight into the relative contributions of the microscopic charge distribution, the geometry of the DNA-solvent interface [6], and the dynamics of water and solvent ions [14,19,20] in intermolecular interactions [21,22].

We thank John Barach for insightful comments. This research was supported in part by the Office of Naval Research through Contract No. ONR-N00014-91-0109.

[1] T. L. Hill, Arch. Biochem. Biophys. **57**, 229 (1955).
[2] A. Katchalsky, Pure Appl. Chem. **26**, 327 (1971).
[3] J. A. Schellman, Biopolymers **16**, 1415 (1977).
[4] M. Fixman, J. Chem. Phys. **70**, 4995 (1979).
[5] A. Pullman and B. Pullman, Q. Rev. Biophys. **14**, 289 (1981).
[6] B. Jayaram, K. A. Sharp, and B. Honig, Biopolymers **28**, 975 (1989).
[7] M. E. Davis and J. A. McCammon, Chem. Rev. **90**, 509 (1990).
[8] W. Saenger, *Principles of Nucleic Acid Structure* (Springer Verlag, Berlin, 1984).
[9] V. Renugopalakrishnan, A. V. Lakshminarayanan, and V. Sasisekharan, Biopolymers **10**, 1159 (1971).
[10] D. A. Pearlman and S.-H. Kim, Biopolymers **24**, 327 (1985).
[11] S. Arnott and D. W. L. Hukins, Biochem. Biophys. Res. Commun. **47**, 1504 (1972).
[12] G. S. Manning, Q. Rev. Biophys. **11**, 179 (1978); Acc. Chem. Res. **12**, 443 (1979).
[13] M. LeBret and B. Zimm, Biopolymers **23**, 287 (1984).
[14] G. Edwards, G. Ying, and J. Tribble, Phys. Rev. A **45**, R8344 (1992).
[15] D. Hochberg, T. W. Kephart, and G. Edwards, Phys. Rev. E **49**, 851 (1994).
[16] M. J. Lighthill, *Fourier Analysis and Generalized Functions* (Cambridge University Press, Cambridge, England, 1970).
[17] S. M. Lindsay *et al.*, J. Biomol. Struc. Dyn. **7**, 279 (1989).
[18] *Theoretical Biochemistry & Molecular Biophysics, Volume 1: DNA*, edited by D. L. Beveridge and R. Lavery (Adenine, Schenectady, NY, 1991).
[19] B. E. Hingerty, R. H. Ritchie, T. L. Ferrell, and J. E. Turner, Biopoloymers **24**, 427 (1985).
[20] D. W. R. Gruen, S. Marcelja, and B. A. Pailthrope, Chem. Phys. Lett. **82**, 315 (1981).
[21] D. C. Rau, B. Lee, and V. A. Parsegian, Proc. Natl. Acad. Sci. USA **81**, 2621 (1984).
[22] R. Podgornic, D. Rau, and V. A. Parsegian, Macromolecules **22**, 1780 (1989); R. Podgornik and V. A. Parsegian, *ibid.* **23**, 2265 (1990).

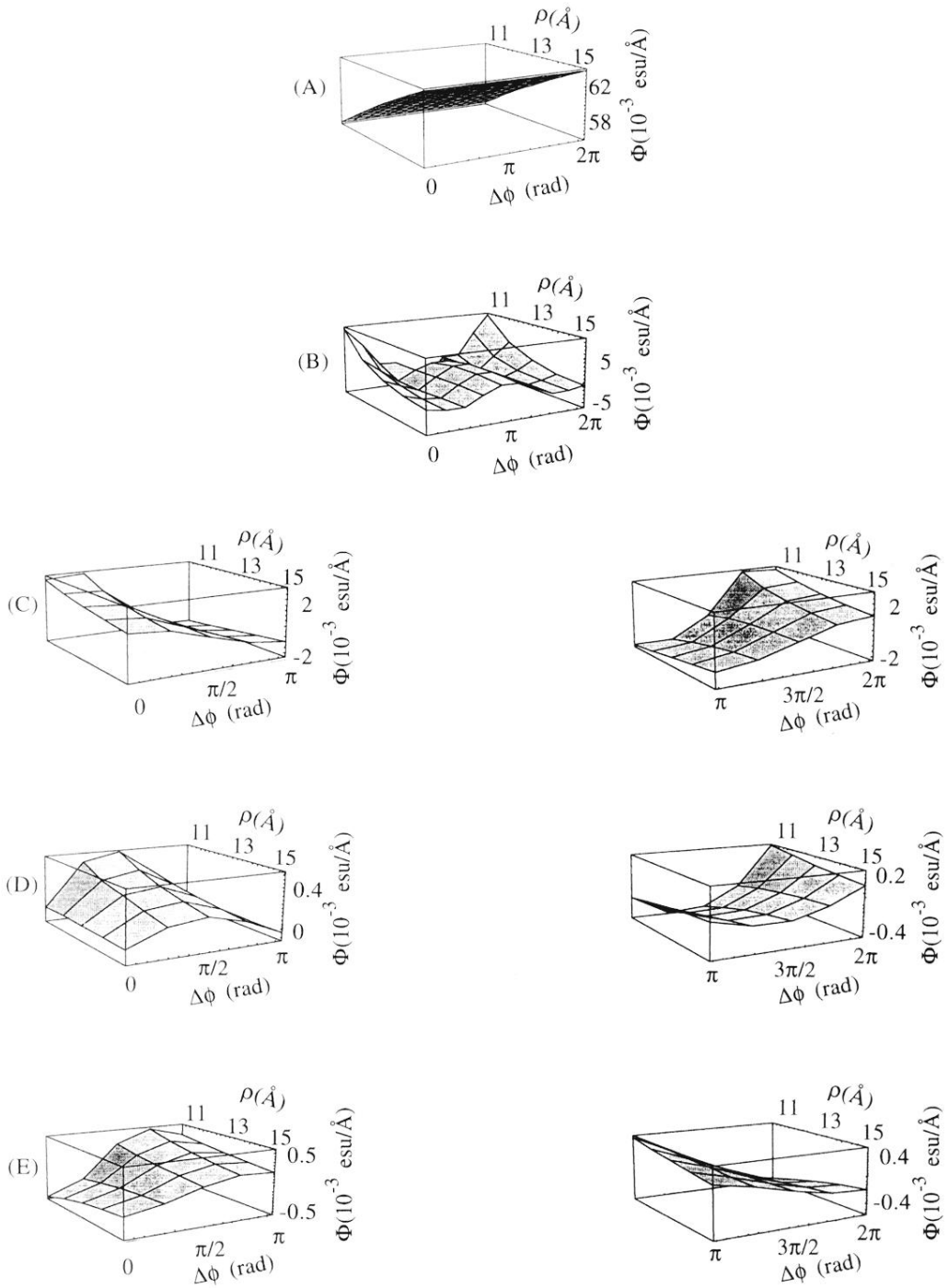


FIG. 2. Surface plots ($z=0$ plane) of the terms comprising the electric potential: (a) zero mode; nonzero mode contributions for the (b) phosphate groups, (c) ribose groups, (d) guanine, and (e) cytosine. Computations were performed as described in Ref. [15]. Note the radius is 1–4 Å from the DNA surface ($b=10$ Å).